

Article

Improved Control Strategy for DFIG Wind Turbines for Low Voltage Ride Through

Zaijun Wu *, Chanxia Zhu and Minqiang Hu

School of Electrical Engineering, Southeast University, No. 2 Sipailou, Nanjing 210096, Jiangsu, China; E-Mails: siyizcx@163.com (C.Z.); mqhu@seu.edu.cn (M.H.)

* Author to whom correspondence should be addressed; E-Mail: zjwu@seu.edu.cn;
Tel.: +86-25-83794163 (ext. 602); Fax: +86-25-83791696.

Received: 20 November 2012; in revised form: 20 February 2013 / Accepted: 20 February 2013 /
Published: 25 February 2013

Abstract: This paper presents an improved control strategy for both the rotor side converter (RSC) and grid side converter (GSC) of a doubly fed induction generator (DFIG)-based wind turbine (WT) system to enhance the low voltage ride through (LVRT) capability. Within the proposed control strategy, the RSC control introduces transient feed-forward compensation terms to mitigate the high frequency harmonic components and reduce the surge in the rotor currents. The proposed GSC control scheme also introduces a compensation term reflecting the instantaneous variation of the output power of the rotor side converter with consideration of the instantaneous power of grid filter impedance to keep the dc-link voltage nearly constant during the grid faults. To provide precise control, non-ideal proportional resonant (PR) controllers for both the RSC and GSC current regulation are employed to further improve dynamic performance. Simulations performed in Matlab/Simulink verify the effectiveness of the proposed control strategy.

Keywords: doubly fed induction generator (DFIG); low voltage ride through (LVRT); grid defaults

1. Introduction

Wind energy generation has been noted as the most rapidly growing renewable energy technology. The increasing penetration level of wind energy can have a significant impact on the grid, especially under abnormal grid voltage conditions. Thus, the power grid connection codes in most countries

require that wind turbines (WTs) should participate in grid voltage support in steady state and remain connected to the grid to maintain the reliability during and after a short-term fault [1]. The latter requirement means that WTs have low voltage ride through (LVRT) capability and supply reactive currents to the grid as stated in the grid codes (e.g., the German E.ON [2], the United States' FERC [3]).

Among the wind turbine concepts, the doubly fed induction generator (DFIG) is a popular wind turbine system due to its high energy efficiency, reduced mechanical stress on the wind turbine, separately controllable active and reactive power, and relatively low power rating of the connected converter [4], but due to the direct connection of the stator to the grid, the DFIG suffers from a great vulnerability to grid faults [5]. There are two main problems that must be overcome to meet the LVRT requirements of DFIGs during voltage sags. The first one is the over-current induced in the rotor circuit of the DFIG, which may damage the rotor side converter (RSC), and the second one is the dc-link over-voltage. Both of them can be attributed to the excessive energy that cannot be transmitted into the grid during the faults [6]. Hence, special countermeasures must be taken to safeguard them against various voltage sag conditions.

Quite a few studies have been carried out to improve the LVRT capability of DFIG WT. Among the available approaches, protection devices such as crowbars are mostly used to bypass the rotor side converter once overloads are detected [7–9]. However, once the crowbar is enabled, the machine controllability will be lost and DFIG becomes a regular induction machine. In this case, instead of providing reactive power support to the grid, the generator absorbs large amounts of reactive power from the grid, which is not conducive to the grid recovery. There are other proposed solutions for fault ride through of DFIG using additional hardware like a series dynamic resistance in the rotor [10] and the stator [11], or using a series line side converter (LSC) topology as proposed in [12]. The use of a dynamic voltage restorer and superconducting fault-current limiter-magnetic energy storage system to enhance the LVRT capability of DFIG during grid faults were also investigated recently in [13,14], respectively. However, these approaches require installing extra hardware in the DFIG WT system, which will increase the costs and decrease the system reliability.

To enhance the LVRT capability of DFIG, steady analysis of DFIGs during grid voltage dips and appropriate control strategies have been proposed to avoid additional hardware in the system. In [15], the RSC is controlled to weaken the effect of the dc and negative sequence components in the stator-flux linkage, thus the rotor current is to be kept within acceptable limits during grid voltage dips. In [16], a dual rotor current controller based on positive and negative reference frames is employed. In [17] a rotor current control scheme based on a main controller implemented in the positive synchronous frame and an auxiliary controller in the negative synchronous frame under unbalanced network conditions is introduced. However, for all the above studies, to obtain the dc, positive and negative sequence components, decomposition of the sequence components and low pass filters are required, which can degrade the system's dynamic response and stability due to the delay and errors introduced during the decomposition process. To improve control dynamic response, proportional integral (PI) plus resonant (R) current regulator [18] and proportional resonant (PR) current regulator [19] are employed in a stator stationary reference frame.

Various studies have also been done on transient analysis in the case of voltage dips [20–22]. However, some of these algorithms are too complicated to implement in industrial applications, and some depend strongly on the proper design of the control parameters or the estimation of certain

parameters, which may have adverse effects on its robustness. In [22], feed-forward transient compensations are added to the conventional current regulator so as to suppress the rotor fault current and enhance the LVRT capability. However, only the RSC was considered, and negative sequence component and dc component also needed to be extracted, thus leading to high computation loads and low response speeds.

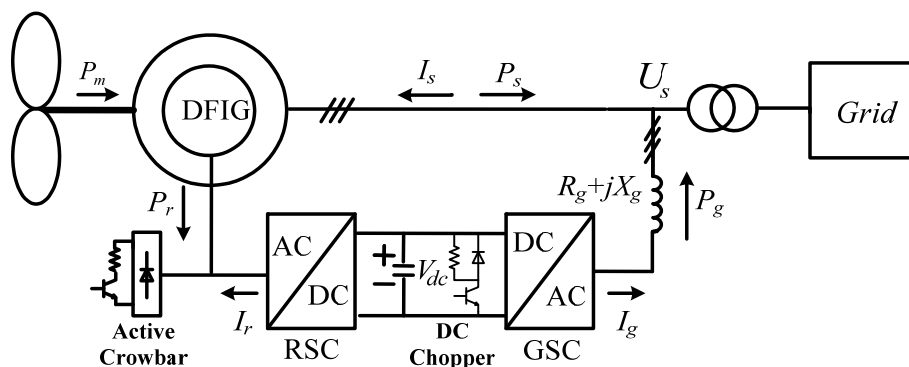
This paper extends the initial study presented in [22] and proposes an improved control strategy for both the RSC and GSC to enhance the LVRT capability of the DFIG WT by suppressing the surge and harmonics in the rotor current and the fluctuation of the dc-link voltage at the same time. To achieve more precise control and better dynamic response, different from the method in [22], proportional resonant (PR) controllers in stationary $\alpha\beta$ reference frame are employed for both the RSC and GSC current regulation. Compared with traditional vector control schemes, the presented RSC control introduces transient compensation terms for eliminating transient errors in the current coupling term during grid faults, whereas the proposed GSC control introduces a compensation term reflecting the instantaneous variation of the output power of the RSC with consideration of the instantaneous power of grid filter impedance.

The paper is organized as follows: Section 2 presents a detailed dynamic model of the DFIG WT system. Section 3 presents a brief theoretical study of the DFIG system under grid faults, with focus on analyzing the rotor current components during unsymmetrical and symmetrical fault conditions. Section 4 proposes the improved control strategy in the RSC and GSC control loop. Section 5 presents a case study using Matlab/Simulink. The simulation results demonstrate the effectiveness of the improved control strategy. Section 6 concludes the analysis.

2. Modeling of the DFIG Wind Turbine

The schematic diagram of a grid-connected DFIG WT system is shown in Figure 1. The DFIG WT system, including the wind turbine, the drive train, the induction generator, a back-to-back voltage source converter with a common dc-link, and the control system, is connected to the grid through a transformer. The back-to-back converters consist of a RSC and a GSC, connected to the grid by a line filter to reduce the harmonics caused by the converters. The main task of the RSC is to control DFIG's stator output active and reactive power, whereas the GSC controls the common dc-link voltage.

Figure 1. Schematic diagram of a grid-connected DFIG WT system.



An active crowbar circuit, which includes a full bridge rectifier, a resistor, and a fully controllable switch, is implemented to protect the RSC from over-current, as shown in Figure 1. Meanwhile, a dc chopper circuit with a 0.5 per unit (pu) resistor is also implemented across the dc bus to protect both the RSC and GSC from dc bus overvoltage.

2.1. Wind Turbine Aerodynamics Model

Due to the short period of time of voltage disturbances, the dynamics of the mechanical part of the turbine will be neglected and the mechanical torque brought in by the wind is assumed to be constant.

2.2. Drive Train Model

In order to study the effects of voltage dips on the mechanical system, the two-mass model of the drive train [23] popularly used to represent dynamic stability of the DFIG WT is given by:

$$\frac{d}{dt} \begin{bmatrix} \Delta\omega_t \\ \Delta\omega_r \\ T_g \end{bmatrix} = \begin{bmatrix} \frac{-D_t - D_{tg}}{2H_t} & \frac{D_{tg}}{2H_t} & \frac{-1}{2H_t} \\ \frac{D_{tg}}{2H_g} & \frac{-D_g - D_{tg}}{2H_g} & \frac{1}{2H_g} \\ K_{tg}\omega_e & -K_{tg}\omega_e & 0 \end{bmatrix} \begin{bmatrix} \Delta\omega_t \\ \Delta\omega_r \\ T_g \end{bmatrix} + \begin{bmatrix} \frac{T_m}{2H_t} \\ \frac{-T_e}{2H_g} \\ 0 \end{bmatrix} \quad (1)$$

where $\Delta\omega_t = \omega_t - \omega_0$, $\Delta\omega_r = \omega_r - \omega_0$ and ω_t , ω_r and ω_0 are the turbine, generator rotor and nominal rotating speed, respectively; T_m and T_e are the mechanical torque of the turbine (here assumed as constant) and the electrical electromagnetic torque of the generator, respectively; T_g is an internal torque of the model; H_t and H_g are the inertia constants of the turbine and the generator, respectively; D_t and D_g are the mechanical damping coefficients of the turbine and the generator, respectively; D_{tg} is the damping coefficient of the flexible coupling (shaft) between the two masses; K_{tg} is the shaft stiffness.

In this paper, the damping coefficient and the shaft stiffness between the turbine and the generator will be ignored, that is, $D_t = D_g = D_{tg} = 0$, $K_{tg} = 0$, $H_t = H_g = H$. Therefore, the Equation (1) becomes the lumped-mass model of the drive train, and the mathematical equation is as follows:

$$T_e = 2H\omega_r + T_m \quad (2)$$

2.3. Induction Generator Model

The voltage equations of the stator and rotor circuits of the induction generator can be expressed in a d - q reference frame rotating at the arbitrary speed as [24]:

$$\begin{cases} u_{ds} = r_s i_{ds} + p\psi_{ds} - \omega\psi_{qs} \\ u_{qs} = r_s i_{qs} + p\psi_{qs} + \omega\psi_{ds} \\ u_{dr} = r_r i_{dr} + p\psi_{dr} - (\omega - \omega_r)\psi_{qr} \\ u_{qr} = r_r i_{qr} + p\psi_{qr} + (\omega - \omega_r)\psi_{dr} \end{cases} \quad (3)$$

$$\begin{cases} \psi_{ds} = L_s i_{ds} + L_m i_{dr} \\ \psi_{qs} = L_s i_{qs} + L_m i_{qr} \\ \psi_{dr} = L_m i_{ds} + L_r i_{dr} \\ \psi_{qr} = L_m i_{qs} + L_r i_{qr} \end{cases} \quad (4)$$

where ψ , u and i represent the flux, voltage and current vectors, respectively. Subscripts s and r denote the stator and rotor quantities, respectively. Subscripts d , q denote q -, and d -axis components, respectively. ω_s and ω_r are the stator, and rotor angular frequencies, respectively. ω is the speed of d - q reference frame. L_s , L_r are the stator and rotor self inductances, respectively, and L_m is the mutual inductance. Also, r_s and r_r are the stator and rotor resistances, respectively. p is the differential operator.

3. Behavior of the DFIG during Grid Faults

When a short-circuit fault occurs in the power grid, the bus voltage at the point of common coupling (PCC) drops, therefore introducing undesirable transients in the stator and rotor currents. The low voltage also prevents the full transmission of generated active power into the grid from DFIG WT, leading to significantly increased fluctuations of the dc-link voltage.

Under unsymmetrical grid fault scenarios, the negative sequence stator currents form a clockwise rotating magnetic motive force (MMF) in the machine air gap. This MMF will then induce a clockwise rotating flux in the gap, which in turn induces an electromotive force (EMF) in the rotor circuit with a frequency of $(2 - s)\omega_s$. Hence, the induced component in the rotor currents has a frequency of $(2 - s)f_s$ as well, where s is the slip ratio, $s = (\omega_s - \omega_r)/\omega_s$. The more severe the unsymmetrical condition at the stator side, the higher will be the magnitude of the rotor current harmonics, which in turn will lead to the harmonics in the electromagnetic torque.

Under symmetrical grid fault scenarios, the stator voltages experience a sudden drop. The relationship of the stator voltage and the stator flux is based on Faraday's law. For each phase, the following equation is given:

$$u_{sj} = r_s i_{sj} + \frac{d\psi_{sj}}{dt} \quad (5)$$

Hence:

$$\psi_{sj} = \int (u_{sj} - r_s i_{sj}) dt \quad (6)$$

where j can be a , b or c .

The EMF induced from the stator flux also experiences a sudden drop. The sudden drop can be seen as an impulse; hence the stator flux will have a dc component. Due to the resistance in the circuit, this dc component will decay. The dc flux component "seen" by the rotor is a rotating magnetic flux with a frequency of f_m (rotating speed). This transient dc component in flux linkage will induce an EMF in the rotor circuits, and a surge of rotor current with a frequency of f_m as well.

Thus, during fault scenarios, the rotor current of DFIG can rise to a high level and the converters in the DFIG system could be damaged, which have relatively lower power rating compared with the WT with fully rated converters. To fulfill the LVRT requirement for DFIG WTs, there are two major issues to be addressed properly under a fault condition. The first one is the over-current which may occur in

the rotor circuit, while the second one is the dc-link voltage fluctuation. Typically, the rotor current limit is 2 pu and the dc-link voltage limit is 1.2 times its nominal value [15].

4. Proposed Low Voltage Ride Through Control Strategy

4.1. Control of Rotor Side Converter

The rotor current control is to mitigate the impact of negative sequence component in the stator current under unsymmetrical grid faults and the surge due to dc component in the stator flux under symmetrical grid faults. These two components will contribute to the large magnitudes of the rotor currents and may damage the power converters for overload capability.

From Equations (3) and (4), the relationship between u_{qr} , u_{dr} and i_{qr} , i_{dr} in the arbitrary rotating dq reference frame can be described as:

$$\begin{bmatrix} u_{dr} \\ u_{qr} \end{bmatrix} = \begin{bmatrix} r_r + L_r' p & -(\omega - \omega_r) L_r' \\ (\omega - \omega_r) L_r' & r_r + L_r' p \end{bmatrix} \begin{bmatrix} i_{dr} \\ i_{qr} \end{bmatrix} + \frac{L_m}{L_s} \begin{bmatrix} u_{ds} \\ u_{qs} - \omega_r \psi_{ds} \end{bmatrix} \quad (7)$$

where L_r' is the rotor transient inductance, $L_r' = \sigma L_r$ with $\sigma = 1 - L_m^2 / L_s L_r$.

In the conventional RSC vector control scheme, the synchronous rotating dq reference frame with the d -axis oriented with the stator-flux vector is employed, where $\omega = \omega_s$, $u_{ds} = 0$ and $u_{qs} = \omega_s \psi_{ds}$. Thus, the relationship between u_{qr} , u_{dr} and i_{qr} , i_{dr} in the synchronous rotating dq reference frame with the d -axis oriented with the stator-flux vector can be derived from Equation (7):

$$\begin{cases} u_{dr} = r_r i_{dr} + \sigma L_r i_{dr} - (\omega_s - \omega_r) \sigma L_r i_{qr} \\ u_{qr} = r_r i_{qr} + \sigma L_r i_{qr} + (\omega_s - \omega_r) \sigma L_r i_{dr} + (\omega_s - \omega_r) \frac{L_m}{L_s} \psi_{ds} \end{cases} \quad (8)$$

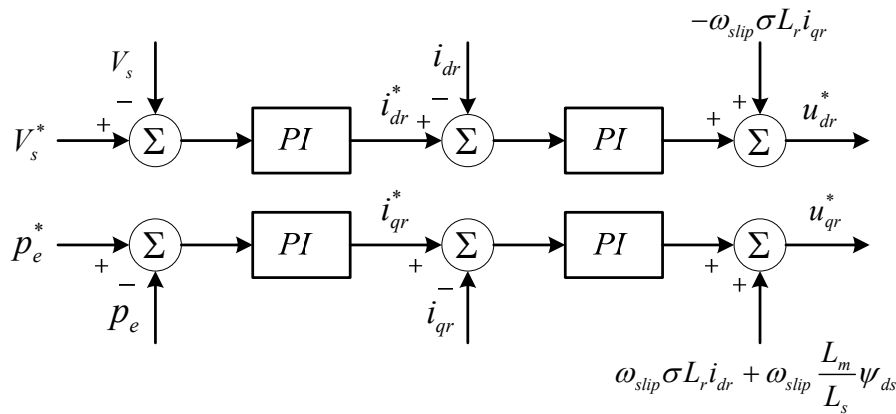
According to Equation (8), there is a cross-coupling item $(\omega_s - \omega_r) \sigma L_r i_{dr}$ in the q -axis RSC control loop while there is another cross-coupling item $(\omega_s - \omega_r) \sigma L_r i_{qr}$ in the d -axis RSC control loop. To decouple d -, q -axis rotor currents control, the feed-forward compensation (FFC) terms u_{qr2} and u_{dr2} are introduced and added to the output of the current regulator:

$$\begin{cases} u_{dr2} = -\omega_{slip} \sigma L_r i_{qr} \\ u_{qr2} = \omega_{slip} \sigma L_r i_{dr} + \omega_{slip} \frac{L_m}{L_s} \psi_{ds} \end{cases} \quad (9)$$

where $\omega_{slip} = \omega_s - \omega_r$.

The conventional RSC control loops with FFC terms are shown in Figure 2, in which the stator output active power (or electromagnetic torque) only relates to the q -axis rotor current and the stator output reactive power (or terminal voltage) only relates to the d -axis rotor current. Typical PI controllers are used in the outer loops for the active and reactive power regulation, and in the inner loops for the rotor currents regulation. Both the outer loops and inner loops apply negative feedback control.

Figure 2. Conventional control scheme for the rotor side converter with FFC.



The aforementioned FFC scheme is assumed that the rotating speed ω of the dq reference frame oriented with the stator flux vector is equal to the synchronous speed ω_s . During steady state, the assumption holds. However, during stator voltage transients, the rotating speed of the stator flux is different from that of the stator voltage space vector [25]. Hence, ω is not necessarily equal to the synchronous speed.

Considering the stator flux transient during grid voltage dips, the DFIG transient model given by Equation (7) should be used instead of Equation (8). Therefore, for more precise control, the transient feed-forward compensation terms u_{qr2} and u_{dr2} should be introduced as [22]:

$$\begin{cases} u_{dr2} = -(\omega - \omega_r)\sigma L_r i_{qr} + \frac{L_m}{L_s} u_{ds} \\ u_{qr2} = (\omega - \omega_r)\sigma L_r i_{dr} + \frac{L_m}{L_s} (u_{qs} - \omega_r \psi_{ds}) \end{cases} \quad (10)$$

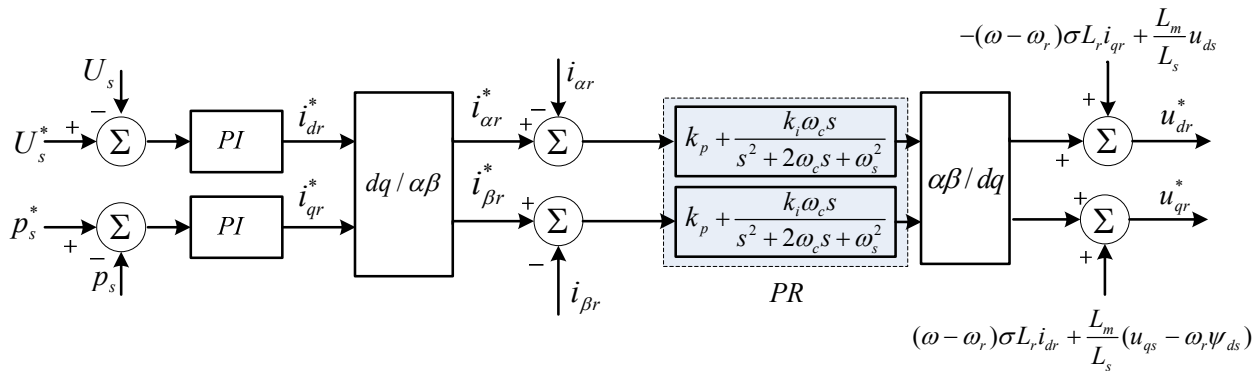
In the typical DFIG RSC control scheme using PI controllers [16], dual current regulators, one for the positive sequence and the other for the negative sequence, were used, in which multiple low pass filters and reference frames transformations are used for extract the dc signals corresponding to the positive sequence, negative sequence, and dc stator flux related components. The multiple filters and the transformations between reference frames will introduce time delay, resulting in amplitude and phase errors. Consequently, the systems cannot be fully decoupled during transients, degrading system dynamic response and stability.

To further improve the dynamical performance of the RSC control, a non-ideal PR regulator tuned at the grid frequency ω_s , illustrated by dashed box in Figure 3, is introduced in the RSC control loop. Compared to ideal PR controller, the gain of non-ideal PR controller is finite, but still relatively high for enforcing small steady-state error, but its bandwidth can be widened by setting ω_c appropriately, which can be helpful for reducing sensitivity towards slight frequency variation in a typical utility grid fault.

The PR controller, which functions as ac PI controllers to track the ac reference value, is implemented in the $\alpha\beta$ stationary reference frame. It is obvious that, in the $\alpha\beta$ stationary reference frame, the positive and negative sequence rotor currents in DFIG will be observed as ac components with the frequency of ω_s and $-\omega_s$, and the dc stator flux related component will be observed as a dc

component. A resonant controller tuned at ω_s is capable of simultaneously regulating the both positive and negative sequence currents at ω_s and $-\omega_s$ in the $\alpha\beta$ reference frame, and even providing zero steady-state error for them [26]. As a result, the proposed PR current controller in the $\alpha\beta$ reference frame can directly regulate the negative sequence components as precisely as the positive sequence without a notch filter for current decomposition, which leads to a better transient response and a fairly simple RSC control design.

Figure 3. Improved control scheme for the rotor side converter with transient FFC.

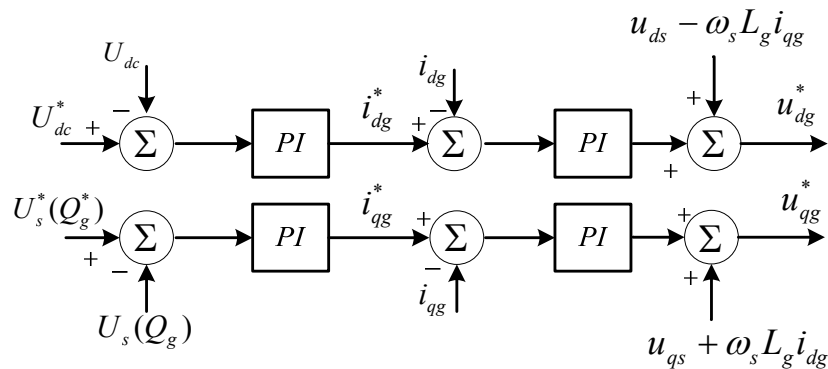


4.2. Control of Grid Side Converter

The grid side converter control is to keep the dc-link voltage constant. When the grid voltage dips, the dc-link voltage may fluctuate due to the instantaneous unbalanced power flow between the grid and rotor side converter. To reduce the fluctuation of dc-link voltage, the item reflecting the instantaneous variation of the output power of the rotor side converter should be introduced during grid faults.

Figure 4 shows the block diagram of the conventional control strategy for the GSC implemented in synchronous rotating dq reference frame with its d -axis oriented with the grid voltage (stator voltage) vector. In order to obtain independent control of active and reactive power flow between the grid and the grid side converter, the PI regulators with cascade control loops are employed in the GSC control scheme, in which the outer control loops are for dc-link voltage and grid reactive power regulation, and the inner control loops are for grid side inductor current regulation.

Figure 4. Conventional control scheme for the grid side converter.



In normal operation, the power flowing through the grid and rotor side converters is balanced, that is, P_r is equal to P_g , so the dc-link voltage is constant. When the grid voltage dips, P_r may not be equal to P_g due to the instantaneous unbalanced power flow between the grid and rotor side converters, and therefore the dc-link voltage may fluctuate.

In [27], a control strategy for limiting the dc-link voltage fluctuation has been applied on the GSC. However, it ignores the power exchanged with the grid filter impedance. For high-power DFIGs, the interface grid side filter reactors are relatively large and cannot be ignored in the model [28]. This section proposes a modified control scheme to limit the dc-link voltage fluctuation during grid faults.

The grid side filter, as shown in Figure 1, suppresses the harmonics caused by the converter, and its dynamics in the synchronous rotating dq reference frame is described by:

$$\begin{cases} u_{dg} = u_{ds} + R_g i_{dg} + L_g \frac{di_{dg}}{dt} - \omega_s L_g i_{qg} \\ u_{qg} = u_{qs} + R_g i_{qg} + L_g \frac{di_{qg}}{dt} + \omega_s L_g i_{dg} \end{cases} \quad (11)$$

where R_g and L_g are the grid side filter resistor and inductor, respectively, and u_{ds} , u_{qs} , u_{dg} , u_{qg} and i_{dg} , i_{qg} are d -axis, q -axis components of the DFIG terminal voltage and grid side filter voltage and current, respectively. u_g is the control voltage provided by the GSC.

According to Equation (11), there is a cross-coupling item $\omega_s L_g i_{dg}$ in the q -axis GSC control loop, while there is another cross-coupling item $\omega_s L_g i_{qg}$ in the d -axis GSC control loop. To decouple the q -axis and d -axis current control in the GSC control loop, the feed-forward compensation terms u_{dg2} and u_{qg2} are introduced as follows:

$$\begin{cases} u_{dg2} = u_{ds} - \omega_s L_g i_{qg} \\ u_{qg2} = u_{qs} + \omega_s L_g i_{dg} \end{cases} \quad (12)$$

Also, the dynamics of the capacitor in the dc-link between the rotor and stator side converters are described by:

$$\begin{cases} C_{dc} V_{dc} \frac{dV_{dc}}{dt} = P_r - P_g \\ P_r = \frac{1}{2} (u_{qr} i_{qr} + u_{dr} i_{dr}) \\ P_g = \frac{1}{2} (u_{qg} i_{qg} + u_{dg} i_{dg}) \end{cases} \quad (13)$$

where C_{dc} is the dc capacitor; V_{dc} is the voltage of the capacitor; P_r and P_g are the instantaneous active power at the RSC and GSC side, respectively.

Because the terminal voltage u_s of the DFIG is oriented with the d -axis, the d -, q -axis voltages become: $u_{ds} = u_s$, $u_{qs} = 0$. Substituting Equation (11) into Equation (13) yields the instantaneous grid side converter active power as:

$$P_g = u_{ds} i_{dg} + R_g i_{dg}^2 + R_g i_{qg}^2 + \frac{1}{2} L_g \frac{di_{dg}^2}{dt} + \frac{1}{2} L_g \frac{di_{qg}^2}{dt} \quad (14)$$

Also, from Equations (13) and (14), the dc-link voltage dynamic equation, in terms of grid side filter current and terminal voltage, can be expressed as:

$$\frac{1}{2}C_{dc} \frac{dV_{dc}^2}{dt} = P_r - (u_{ds}i_{dg} + R_g i_{dg}^2 + R_g i_{qg}^2 + \frac{1}{2}L_g \frac{di_{dg}^2}{dt} + \frac{1}{2}L_g \frac{di_{qg}^2}{dt}) \tag{15}$$

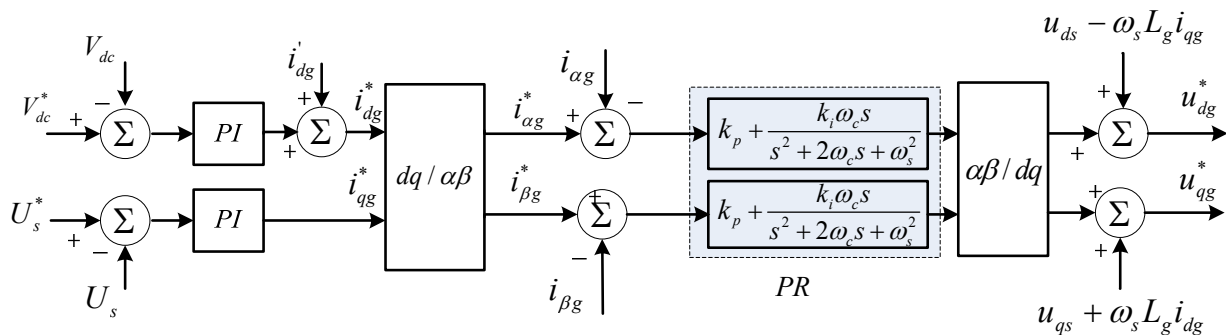
During grid voltage dips, the variation of the output power of the rotor side converter leads to the imbalance of active power between the grid and rotor side converters, and therefore the dc-link voltage may fluctuate. If the grid filter active current reference during voltage dips is determined so that the sum of instantaneous powers of the GSC and the grid filter is nearly equal to the instantaneous output power of the RSC, the dc-link voltage will not change significantly and will remain nearly constant.

Since the GSC rating is limited, the priority is given to the dc-link voltage control. Thus, the term i'_{dg} described by Equation (16) is represented as a disturbance to compensate the instantaneous RSC power in the GSC control scheme. In such a way, the smaller dc-link voltage fluctuation can be achieved during grid voltage dips:

$$P_r = u_{ds}i'_{dg} + R_g i_{dg}^2 + \frac{1}{2}L_g \frac{di_{dg}^2}{dt} \tag{16}$$

Like in the RSC control design, PR controllers are also applied to the GSC control loop to improve dynamic response. The improved GSC control loops are shown in Figure 5, in which the *d*-axis reference current (active current reference) of the grid side converter is set as the output of the dc-link voltage controller. Also, the *q*-axis reference current (reactive current reference) is used for the terminal voltage control.

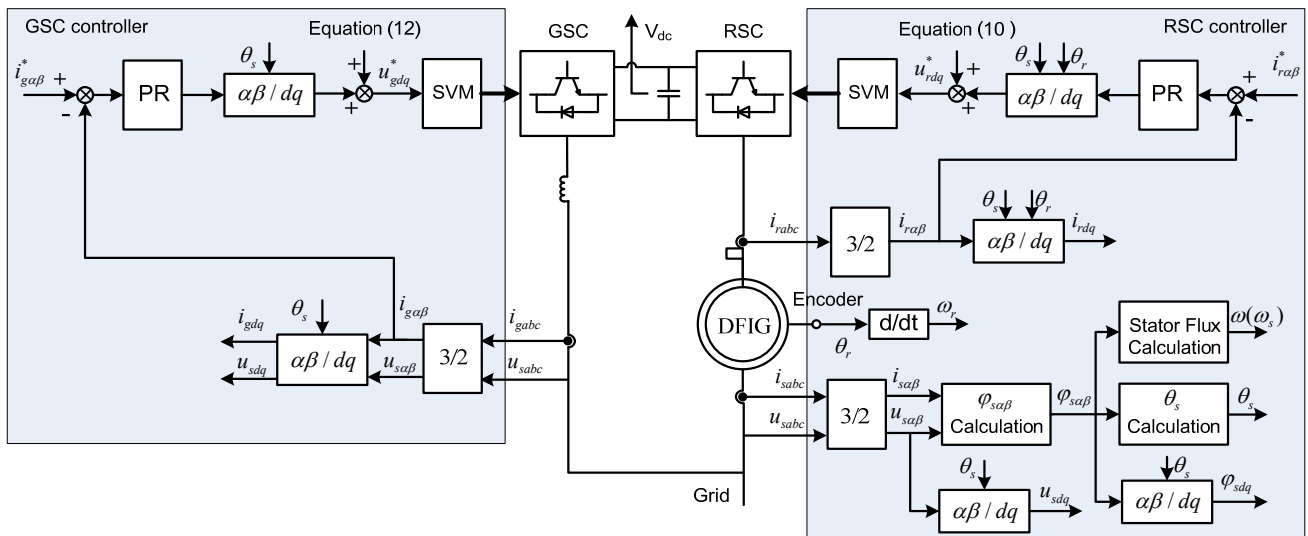
Figure 5. Improved control scheme for the grid side converter with transient FFC.



4.3. System Implementation

Figure 6 shows the implementation of the proposed controllers for the RSC and GSC. As shown, the measured three-phase currents are directly transformed into the $\alpha\beta$ reference frame, without being decomposed separately into the positive and negative sequence components, thus improving the control system dynamic response during grid faults.

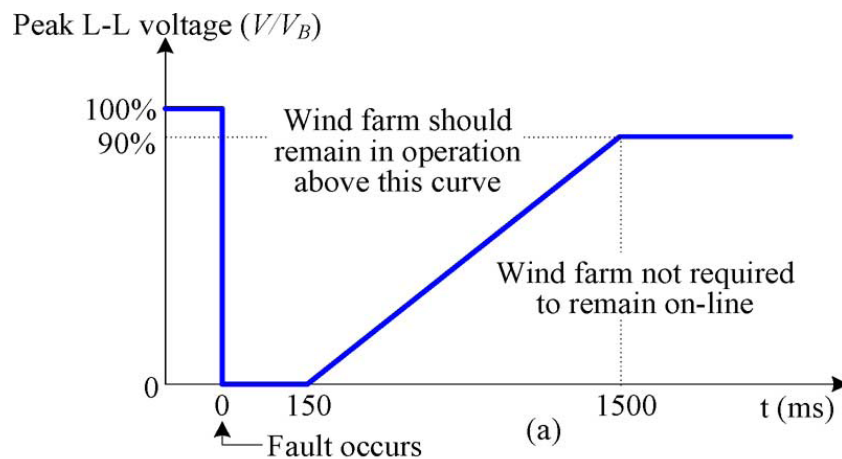
Figure 6. Schematic diagram of the proposed current controllers for the GSC and RSC.



5. Simulation Results

In this paper, LVRT requirement enforced by the E.ON grid code [2] is considered. As shown in Figure 7, the wind farms must stay in operation as long as the voltage at the grid connection point remains above the solid line. According to Figure 6, wind farms must withstand voltage drops down to 0% of the nominal voltage at the point of common coupling for durations up to 150 ms.

Figure 7. LVRT requirement during grid fault following E.ON code.



In order to validate the effectiveness of the proposed control strategy, simulation studies using Matlab/Simulink have been conducted on a 2 MW DFIG WT. The DFIG is connected to a grid (infinite bus) through the line filter, as shown in Figure 1. The parameters of the system are listed in Table 1. The nominal converter dc-link voltage is 1200 V and PWM with a switching frequency of 3 kHz is used for both the RSC and GSC. The crowbar resistor is chosen to be 0.5 pu [8], and the chopper circuit resistor is 0.5 pu.

Table 1. Parameters of a single 2 MW DFIG and the network system.

Rated power	2 MW
Rated voltage	690 V
R_s	0.00059 pu
X_s	0.01350 pu
R_r	0.00339 pu
X_r	0.00750 pu
X_M	0.41610 pu
Z_g	0.02 + j0.3 pu
H	5.0 s

In the following analyses, to examine the dynamic behaviors of DFIG WT with the proposed control strategy to meet the LVRT requirement of E.ON, two typical short-circuit faults, say symmetrical and unsymmetrical faults, are imposed on the transmission power grid, causing the voltage at PCC to drop to 0% for 500 ms, respectively. Two different control strategies for LVRT of the studied DFIG WT are investigated and compared under an unsymmetrical fault scenario and a symmetrical fault scenario, including:

(1) Strategy A (Conventional control strategy): standard PI controller ($K_p = 3$, $K_i = 100$) is applied to the RSC and GSC control loops with FFC. The simulation results are indicated with the blue line in Figures 8 and 9.

(2) Strategy B (Proposed control strategy): non-ideal PR controller ($K_p = 3$, $K_i = 100$, $\omega_c = 5$ rad/s) is applied to the RSC and GSC control loops with transient FFC. The simulation results are indicated with the black line in Figures 8 and 9.

5.1. Unsymmetrical Fault Scenario

At time $t = 1.0$ s, a single-phase to ground short-circuit fault in phase A occurs in the power grid. During the fault, the voltage at PCC drops to zero with duration of 500 ms. The transient behaviors of the studied DFIG WT with different control strategies are simulated and compared, respectively.

Figure 8 shows the dynamic responses of the studied system during this fault, but with two different control schemes. The simulation results in Figure 8 show that the rotor current and dc-link voltage can be kept below the safety limits for the both control schemes. However, with the improved control strategy, the high frequency harmonics in the rotor currents and the torque can be effectively suppressed. Also, from Figure 8, it is found that, with the improved control scheme, the ripple of the dc-link voltage can be reduced more effectively compared with the conventional control scheme.

Figure 8 also shows a comparison of the rotor voltage for two different control strategies in *abc* reference frame. It is found that the rotor voltages are more unbalanced for the proposed control strategy. This is due to the increased negative sequence compensation from the RSC. In other words, the cost of good suppression is a larger magnitude in the injected rotor voltages.

Figure 8. Dynamic responses of the studied DFIG WT during a single-phase to ground fault when the voltage at PCC drops to zero for 500 ms; (a) full time scale from $t = 0$ s to $t = 2.0$ s; (b) zooming from $t = 1.1$ s to $t = 1.3$ s.

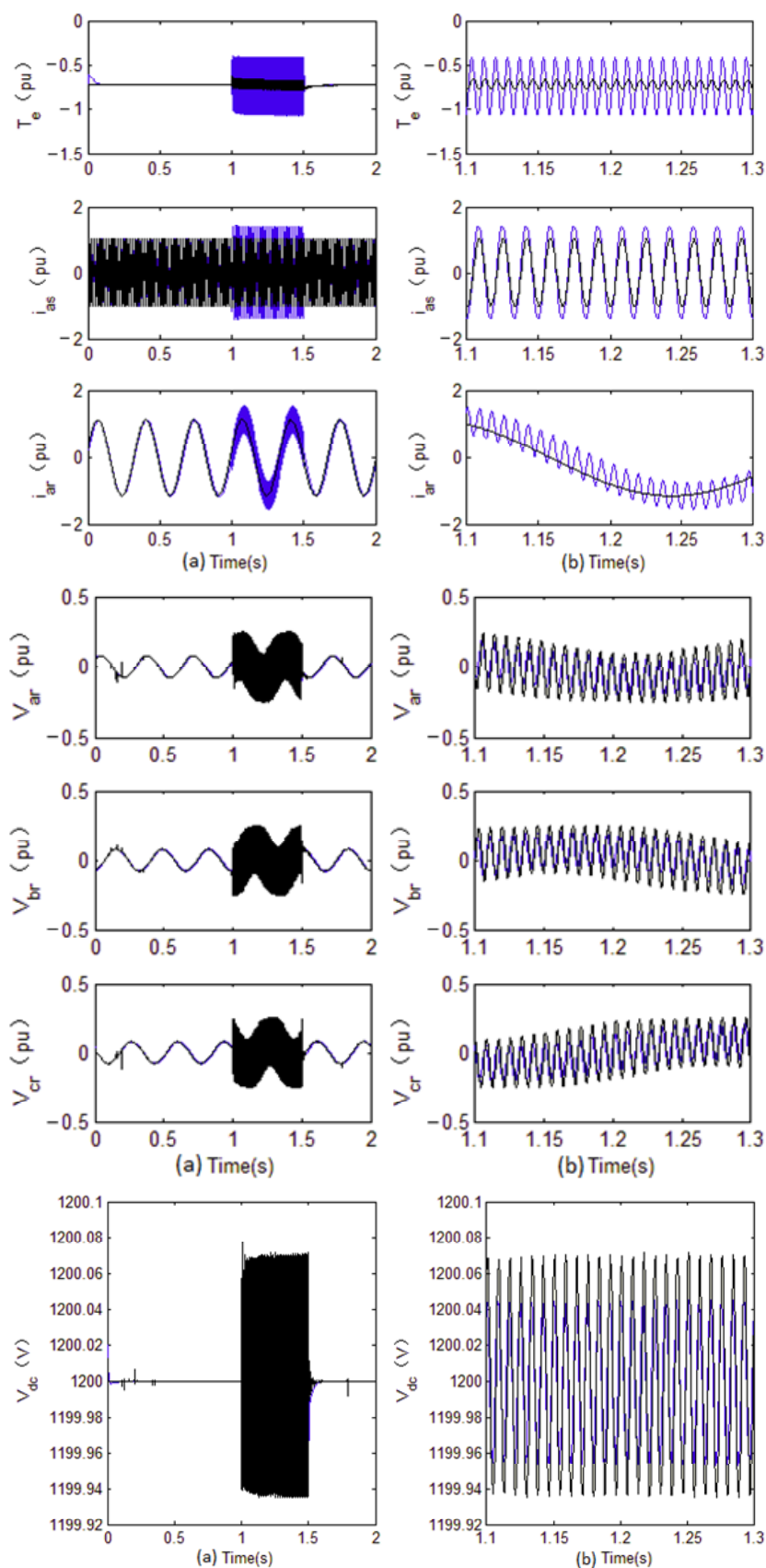
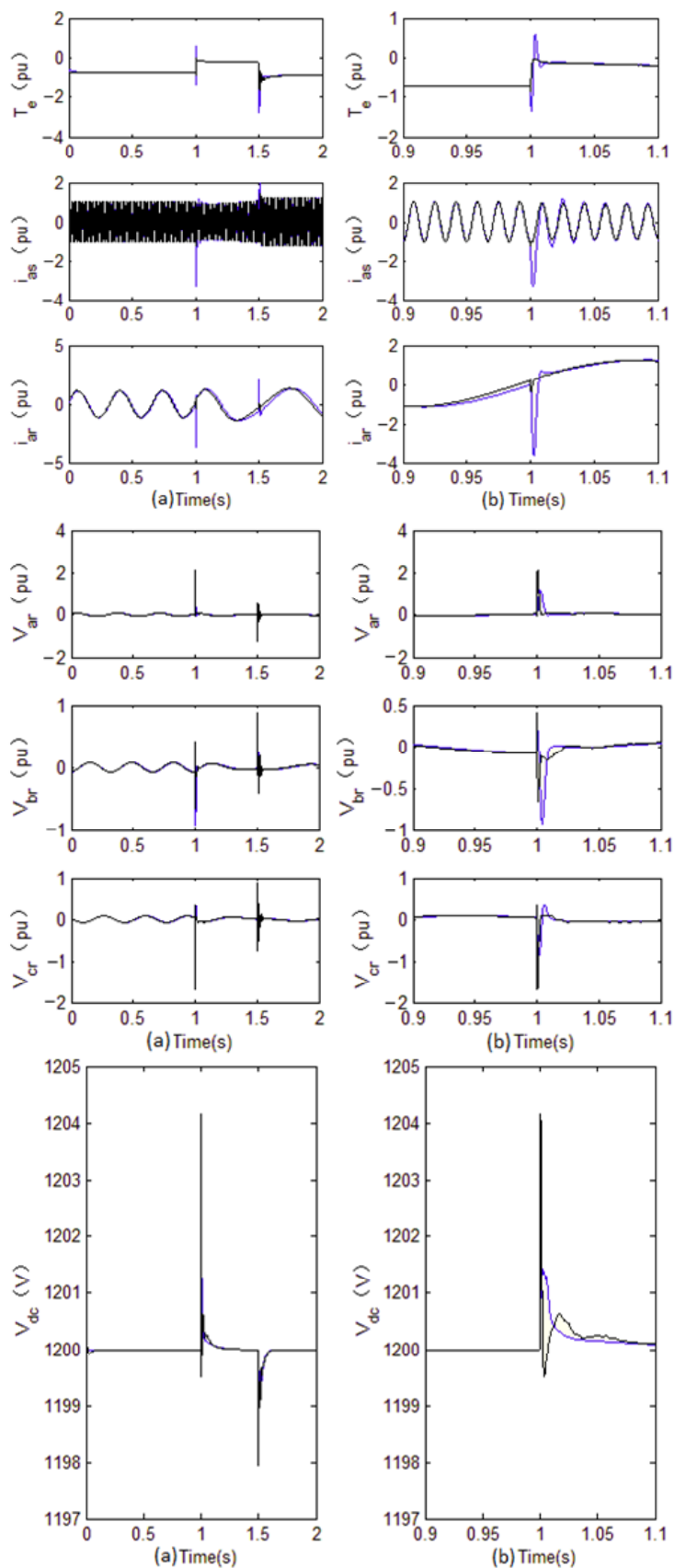


Figure 9. Dynamic responses of the studied DFIG WT during a three-phase short-circuit fault when the voltage at PCC drops to zero for 500 ms, (a) full time scale from $t = 0$ s to $t = 2.0$ s; (b) zooming from $t = 0.9$ s to 1.1 s.



5.2. Symmetrical Fault

To verify the effectiveness of the proposed control strategy under symmetrical fault conditions, another simulation of severe balanced sag has been performed. At time $t = 1.0$ s, a three-phase short-circuit fault occurs in the power grid. During the fault, the voltage at PCC drops to zero with duration of 500 ms. The transient behaviors of the studied DFIG WT with different control strategies are simulated and compared, respectively.

From the simulation results in Figure 9, it can be found that with the conventional PI current regulator, the transient dc component of the stator flux causes a surge of the rotor current, which will exceed the RSC safety limit and damage the RSC, while with the improved control strategy, the surge current in the rotor circuit can be suppressed effectively even under this extreme case. Consequently, the electromagnetic torque overshoots are notably decreased, which ensures less mechanical stress imposed on bearing of the turbine shaft. Also, with the improved control strategy, the dc-link voltage can be controlled effectively to keep below the safety limit. Figure 9 also shows the dynamic response of the rotor voltage. It is found that the rotor voltage can be kept below the safety limits since the proposed control strategy prevents large inrush currents in the rotor winding.

6. Conclusions

In this paper, an improved control strategy for both the RSC and GSC of a DFIG WT system has been proposed to enhance low voltage ride through capability. The proposed control strategy introduces the transient feed-forward compensation terms in the RSC control loops and the instantaneous rotor power fluctuation compensate terms in the GSC control loops, which are derived from the accurate transient control model of DFIG WT system. In addition, PR controllers are employed for both the RSC and GSC current control loop to further improve system dynamic response. Simulation results confirmed the effectiveness of the proposed control strategy with reduced harmonics in the rotor currents, electromagnetic torque and fluctuation of the dc-link voltage during both the unsymmetrical and symmetrical grid faults. Compare with the conventional control strategy, the DFIG WT installed with the proposed control strategy gives a better transient behavior with little additional computation effort.

Acknowledgments

This paper is supported in part by grants from National Natural Science Foundation of China (project No. 51177015), and the National High Technology Research and Development program of China (863 Program) (Project No. 2011AA05A107).

References

1. Tsili, M.; Papathanassiou, S. A review of grid code technical requirements for wind farms. *IET Renew. Power Gen.* **2009**, *3*, 308–332.
2. Erlich, I.; Winter, W.; Dittrich, A. Advanced Grid Requirements for the Integration of Wind Turbines into the German Transmission System. In *Proceedings of IEEE Power Engineering Society General Meeting 2006*, Montreal, Quebec, Canada, 18–22 June 2006.

3. Federal Energy Regulatory Commission. Regulatory Order No. 661-A: Interconnection for Wind Energy. Available online: <http://www.ferc.gov/industries/electric/indus-act/gi/wind.asp> (accessed on 21 February 2013).
4. Thomas, A. *Wind Power in Power Systems*; Wiley: New York, NY, USA, 2005.
5. Mohseni, M.; Islam, S.; Masoum, M. Impacts of symmetrical and asymmetrical voltage sags on DFIG-based wind turbines considering phase angle jump, voltage recovery, and sag parameters. *IEEE Trans. Power Electron.* **2011**, *26*, 1587–1598.
6. Yang, L.; Xu, Z.; Ostergaard, J.; Dong, Z.; Wong, K. Advanced control strategy of DFIG wind turbines for power system fault ride through. *IEEE Trans. Power Syst.* **2012**, *27*, 713–722.
7. Zhang, W.; Zhou, P.; He, Y. Analysis of the By-Pass Resistance of an Active Crowbar for Doubly-Fed Induction Generator Based Wind Turbines under Grid Faults. In *Proceedings of International Conference on Electrical Machines and Systems (ICEMS 2008)*, Wuhan, China, 17–20 October 2008.
8. Pannell, G.; Atkinson, D.; Zahawi, B. Minimum-threshold crowbar for a fault-ride-through grid-code-compliant DFIG wind turbine. *IEEE Trans. Energy Convers.* **2010**, *25*, 750–759.
9. Morren, J.; de Haan, S. Ride through of wind turbines with doubly fed induction generator during a voltage dip. *IEEE Trans. Energy Convers.* **2005**, *20*, 35–441.
10. Yang, J.; Fletcher, J.; O'Reilly, J. A series-dynamic-resistor-based converter protection scheme for doubly-fed induction generator during various fault conditions. *IEEE Trans. Energy Convers.* **2010**, *25*, 422–432.
11. Causebrook, A.; Atkinson, D.; Jack, A. Fault ride-through of large wind farms using series dynamic braking resistors. *IEEE Trans. Power Syst.* **2007**, *22*, 966–975.
12. Flannery, P.; Venkataramanan, G. Unbalanced voltage sag ride through of a doubly fed induction generator wind turbine with series grid-side converter. *IEEE Trans. Ind. Appl.* **2009**, *45*, 1879–1887.
13. Wessels, C.; Gebhardt, F.; Fuchs, F.W. Fault ride-through of a DFIG wind turbine using a dynamic voltage restorer during symmetrical and asymmetrical grid faults. *IEEE Trans. Power Electron.* **2011**, *26*, 807–815.
14. Guo, W.; Xiao, L.; Dai, S. Enhancing low-voltage ride-through capability and smoothing output power of DFIG with a superconducting fault-current limiter–magnetic energy storage system. *IEEE Trans. Energy Convers.* **2012**, *27*, 277–295.
15. Xiang, D.; Ran, L.; Tavner, P.J.; Yang, S. Control of a doubly fed induction generator in a wind turbine during grid fault ride-through. *IEEE Trans. Energy Convers.* **2006**, *21*, 652–662.
16. Xu, L.; Wang, Y. Dynamic modeling and control of DFIG-based wind turbines under unbalanced network conditions. *IEEE Trans. Power Syst.* **2007**, *22*, 314–323.
17. Xu, L. Enhanced control and operation of DFIG-based wind farms during network unbalance. *IEEE Trans. Energy Convers.* **2008**, *23*, 1073–1081.
18. Hu, J.; He, Y.; Xu, L.; Williams, B.W. Improved control of DFIG systems during network unbalance using PI-R current regulators. *IEEE Trans. Ind. Electron.* **2009**, *56*, 439–451.
19. Hu, J.; He, Y. Reinforced control and operation of DFIG-based wind power-generation system under unbalanced grid voltage conditions. *IEEE Trans. Energy Convers.* **2009**, *24*, 905–915.

20. Rahimi, M.; Parniani, M. Transient performance improvement of wind turbines with doubly fed induction generators using nonlinear control strategy. *IEEE Trans. Energy Convers.* **2010**, *25*, 514–525.
21. Lima, F.K.A.; Luna, A.; Rodriguez, P.; Watanabe, E.H.; Blaabjerg, F. Rotor voltage dynamics in the doubly fed induction generator during grid faults. *IEEE Trans. Power Electron.* **2010**, *25*, 118–130.
22. Liang, J.; Qiao, W.; Harley, R.G. Feed-forward transient current control for low-voltage ride-through enhancement of DFIG wind turbines. *IEEE Trans. Energy Convers.* **2010**, *25*, 836–843.
23. Fan, L.; Kavasseri, R.; Miao, Z.; Zhu, C. Modeling of DFIG-based wind farms for SSR analysis. *IEEE Trans. Power Deliv.* **2010**, *25*, 2073–2082.
24. Novotny, D.W.; Lipo, T.A. *Vector Control and Dynamics of AC Drives*; Oxford University Press: London, UK, 2000.
25. Zhang, Z.; Xu, L.; Zhang, Y.; Guan, B. Novel Rotor-Side Control Scheme for Doubly Fed Induction Generator to Ride Through Grid Faults. In *Proceedings of Energy Conversion Congress and Exposition (ECCE 2010)*, Atlanta, GA, USA, 12–16 September 2010.
26. Teodorescu, R.; Blaabjerg, F.; Liserre, M.; Loh, P. Proportional resonant controllers and filters for grid-connected voltage-source converters. *IEE Proc. Electr. Power Appl.* **2006**, *153*, 750–762.
27. Yao, J.; Li, H.; Liao, Y.; Chen, Z. An improved control strategy of limiting the DC-link voltage fluctuation for a doubly fed induction wind generator. *IEEE Trans. Power Electron.* **2008**, *23*, 1205–1213.
28. Rahimi, M.; Parniani, M. Coordinated control approaches for low-voltage ride-through enhancement in wind turbines with doubly fed induction generators. *IEEE Trans. Energy Convers.* **2010**, *25*, 873–883.

© 2013 by the authors; licensee MDPI, Basel, Switzerland. This article is an open access article distributed under the terms and conditions of the Creative Commons Attribution license (<http://creativecommons.org/licenses/by/3.0/>).